Atmos. Chem. Phys. Discuss., 4, 3485–3533, 2004
www.atmos-chem-phys.org/acpd/4/3485/
SRef-ID: 1680-7375/acpd/2004-4-3485

Atmospheric Chemistry and Physics Discussions

Simulating the global atmospheric black carbon cycle: a revisit to the contribution of aircraft emissions

J. Hendricks[1], **B. Kärcher**[1], **A. Döpelheuer**[2,*], **J. Feichter**[3], **U. Lohmann**[4], and **D. Baumgardner**[5]

[1]DLR-Institut für Physik der Atmosphäre, Oberpfaffenhofen, Germany
[2]DLR-Institut für Antriebstechnik, Köln, Germany
[*]Now at DLR-Vorstand, Köln, Germany
[3]Max-Planck-Institut für Meteorologie, Hamburg, Germany
[4]Dalhousie University, Halifax, Canada
[5]Centro de Ciencias de la Atmósfera, Universidad Nacional Autonoma de Mexico, Mexico City, Mexico

Received: 19 April 2004 – Accepted: 25 May 2004 – Published: 22 June 2004

Correspondence to: J. Hendricks (johannes.hendricks@dlr.de)

Abstract

The black carbon (BC) burden of the upper troposphere and lowermost stratosphere (UTLS) is investigated with the general circulation model (GCM) ECHAM4. The special focus is the contribution of aircraft emissions to the UTLS BC loading. Previous studies on the role of aircraft emissions in the global BC cycle either neglect BC sources located at the Earth's surface or simplify the BC cycle by assuming pre-defined BC residence times. Here, the global BC cycle including emissions, transport, and removal is explicitly simulated. The BC emissions considered include surface sources as well as BC from aviation. This enables a consistent calculation of the relative contribution of aviation to the global atmospheric BC cycle. As a further extension to the previous studies, the aviation-induced perturbation of the UTLS BC particle number concentration is investigated. Several sensitivity studies were performed to evaluate the uncertainties associated with the model predictions. The simulated UTLS BC concentrations are compared to in-situ observations. The simulations suggest that the large-scale contribution of aviation to the UTLS BC mass budget typically amounts to only a few percent, even in the most frequented flight regions. The aviation impact far away from these regions is negligible. The simulated aircraft contributions to the UTLS BC particle number concentration are much larger compared to the corresponding mass perturbations. The simulations suggest that aviation can cause large-scale increases in the UTLS BC particle number concentration of more than 30% in regions highly frequented by aircraft. The relative effect shows a pronounced annual variation with the largest relative aviation impact occurring during winter.

1. Introduction

Anthropogenic black carbon (BC) emissions cause significant perturbations of the global atmospheric aerosol burden (e.g. Penner et al., 1993; Cooke and Wilson, 1996; Liousse et al., 1996; Cooke et al., 1999, 2002). Different atmospheric impacts of

ACPD

4, 3485–3533, 2004

BC aerosols have been discussed. Important climatic effects due to direct impacts on radiation can be expected (e.g. Schult et al., 1997; Haywood and Ramaswamy, 1998; Myhre et al., 1998; Penner et al., 1998; Cooke et al., 1999; Chung and Seinfeld, 2002; Jacobson, 2002). Additionally, indirect climatic effects due to impacts on cloud droplet number concentration and related cloud properties have been considered (e.g. Lohmann et al., 2000). In the upper troposphere and lowermost stratosphere (UTLS), BC particles may be involved in ice cloud formation and may affect the frequency and optical properties of cirrus clouds (e.g. DeMott et al., 1997; Jensen and Toon, 1997; Petzold et al., 1998; Ström and Ohlsson, 1998; Kärcher, 1999; Gierens, 2003; Kärcher and Lohmann, 2003).

Significant amounts of BC aerosols have been observed in the UTLS (e.g. Pueschel et al., 1992; Blake and Kato, 1995; Baumgardner et al., 2003, 2004). Three-dimensional (3-D) model calculations indicate a significant BC loading of the UTLS (e.g. Cooke and Wilson, 1996; Liousse et al., 1996; Cooke et al., 1999, 2002; Koch, 2001; Köhler et al., 2001; Chung and Seinfeld, 2002). Black carbon aerosols are an important combustion product of aircraft engines (e.g. IPCC, 1999). Therefore, it has been debated whether aviation may contribute significantly to the BC budget of the UTLS region. Danilin et al. (1998) discussed global simulations on the atmospheric dispersion of aircraft fuel tracer emissions performed with different 2-D and 3-D models considering pre-defined tracer lifetimes. From the fuel tracer distributions, the aircraft-induced increase in atmospheric BC mass loading was derived considering typical BC emission indices. Rahmes et al. (1998) performed 2-D simulations on the aircraft contribution to the atmospheric BC mass loading including a detailed representation of processes controlling the atmospheric BC cycle. The Danilin et al. (1998) and Rahmes et al. (1998) model studies reveal maximum zonal mean aircraft-induced perturbations in the range of 0.1–1 ng(BC)/m^3 occurring in the northern mid- and high latitude UTLS. However, since the effect of surface BC emissions on the UTLS region was not included in the models, the relative impact of aviation BC emissions could not be quantified. Detailed knowledge about the total BC loading of the UTLS or about the contribution of

BC from surface sources to the UTLS BC budget is required to evaluate the relative importance of the aviation impact.

Comparing the observational data provided by Pueschel et al. (1992) and Blake and Kato (1995) with the model studies by Danilin et al. (1998) and Rahmes et al. (1998), one finds that the BC concentrations measured in the northern hemispheric mid- and high latitude UTLS are comparable to the simulated aircraft-induced perturbations. However, recent observations by Baumgardner et al. (2003, 2004) reveal that UTLS BC concentrations can be significantly larger than the simulated aviation-induced BC levels. The observational data currently available is too sparse to provide climatological information on the global BC mass budget. Hence, a robust evaluation of the importance of the simulated aviation impact on the basis of observations is currently not possible.

Information on the UTLS background BC concentrations, attributed to BC from surface sources, can be gained from other global model studies focused on the atmospheric dispersion of BC from surface emissions (e.g. Cooke and Wilson, 1996; Liousse et al., 1996; Cooke et al., 1999; Koch, 2001; Cooke et al., 2002; Köhler et al., 2001; Chung and Seinfeld, 2002). The UTLS background BC concentrations simulated with the various models can show large differences. Since also the aviation-induced perturbations simulated with the different model approaches discussed by Danilin et al. (1998) and Rahmes et al. (1998) differ significantly, calculations of the relative impact of aviation should be based on a consistent model approach including both surface BC emissions as well as BC from aviation. The only study analysing the aviation impact with such a consistent approach was provided by Köhler et al. (2001). However, Köhler et al. (2001) stressed that, due to the consideration of pre-defined BC half-lifetimes in their simulations, a reliable quantification of the aviation impact was not possible. This indicates the need for a more physically-based consistent simulation of the respective contributions of aviation and surface sources to the UTLS BC budget.

In the present study, the impact of aircraft activity on the global BC budget is quantified by means of simulations with a general circulation model (GCM) considering both

3-D aircraft BC emissions as well as BC from surface sources. The atmospheric BC cycle including BC emissions, transport, and removal by wet and dry deposition is simulated explicitly. Aircraft-related BC is treated separately from BC particles resulting from surface emissions to track its atmospheric fate. The previous model studies focused on the atmospheric BC mass loading. Given the potential impact of BC particles on ice cloud formation via heterogeneous nucleation, potential aircraft-induced impacts on the BC particle number concentration in the UTLS region are also investigated here. In Sect. 2 and the Appendix, the model is described in detail. Section 3.1 reports on the simulations performed. The major results as well as the uncertainties associated with the model predictions are discussed in Sect. 3.2. The main conclusions are given in Sect. 4.

2. Model description

2.1. General description

The ECHAM4 GCM (Roeckner et al., 1996) is applied. Standard prognostic variables are vorticity, divergence, temperature, (logarithm of) surface pressure, water vapor and cloud water. The model includes physical parameterizations of radiation, cloud processes, precipitation, convection, diffusion, planetary boundary layer dynamics, land-surface processes as well as gravity wave drag. A spectral transform approach with triangular truncation at zonal wave number 30 (T30) is used. This results in a nominal horizontal resolution of approximately 3.75° in latitude and longitude. The model domain covers the vertical range from the surface to 10 hPa using 19 vertical layers characterized by a hybrid σ-p-coordinate system. A semi-implicit leap frog scheme is applied for time integration. A time step Δt of 30 min is used. The horizontal and vertical advection of positive definite quantities like water vapor, cloud water, or trace constituents is calculated applying a semi-Lagrangian scheme (Williamson and Rasch, 1994).

ACPD
4, 3485–3533, 2004

2.2. Aerosols and clouds

The model version employed here includes explicit predictions of cloud water, cloud ice, as well as cloud droplet and ice crystal number concentration (Lohmann and Roeckner, 1996; Lohmann et al., 1999; Lohmann and Kärcher, 2002). The convective transport of trace constituents is treated according to Brinkop and Sausen (1997). Aerosols are represented as described by Feichter et al. (1996) and Lohmann et al. (1999). The aerosol module treats the atmospheric cycles of sulfate aerosols, carbonaceous particles (organic carbon as well as BC), sea-salt, and mineral dust aerosols. Particle mass concentrations of the respective aerosol types are predicted each time step. Emissions of BC particles, representative of the mid-1980s, are considered as described by Cooke and Wilson (1996) resulting in global BC emission rates of 7.96 and 5.98 $TgC\,yr^{-1}$ for BC emissions due to fossil fuel combustion and biomass burning, respectively. The hygroscopic properties of BC particles are represented according to Cooke et al. (1999) assuming that the BC surface emissions can be characterized as 80% hydrophobic and 20% hydrophilic particles and that hydrophobic BC is transformed to hydrophilic BC according to an exponential decay process showing an e-folding time of 24 h. BC is removed from the atmosphere by wet and dry deposition. Dry deposition rates are calculated according to the surface conditions and the BC hygrospcopic properties. Wet deposition occurs via precipitation scavenging of hydrophilic BC. It is assumed that 90% of the in-cloud hydrophilic BC mass is scavenged by cloud droplets. This is consistent with upper limit in-cloud BC scavenging rates reported in the literature (e.g. Hitzenberger et al., 2001). The BC precipitation flux is then calculated from the in-cloud precipitation formation rate as well as from the efficiencies of below-cloud evaporation and below-cloud scavenging of BC by rain or snow. In contrast to Lohmann and Kärcher (2002), the mass scavenging efficiency of hydrophilic aerosols by ice is chosen as 5% instead of 10%. With this modification, the sulfate mass concentrations simulated for the tropopause region are in better agreement with recent observations (Dibb et al., 1998, 2000).

ACPD
4, 3485–3533, 2004

To calculate particle number concentrations from the simulated aerosol mass concentrations, prescribed particle size distributions typical of the respective aerosol type are employed. Lognormal size distributions as described by Köpke et al. (1997) and Hess et al. (1998) are used for each individual aerosol type. Aged BC particles are mostly fractal clusters which can be characterized as long, often multi-connected chains consisting of tiny spherical elements. These spherules are referred to as primary BC particles. Following Köpke et al. (1997), the particle size distribution of the spherules is characterized by a number median diameter of d=0.0236 μm and a geometric standard deviation of σ=2.0. A specific density of the subspheres of 2.3 g cm^{-3} is assumed. The number n of primary particles agglomerated to form an atmospheric BC particle can be highly variable even in the upper troposphere and the stratosphere (e.g. Blake and Kato (1995) or Pueschel et al. (2000) for UTLS BC; Strawa et al. (1999) for stratospheric BC). Observational information on n at these altitudes is too sparse to enable robust assumptions on a representative value of n. The available measurements suggest that n has an order of magnitude of 10–100. However, small BC particles are underrepresented in these measurements. Hence, we assume that BC particles resulting from surface sources contain 10 primary particles on average. With this assumption the BC particle number concentration can be derived from the BC mass concentration. The potential consequences of the choice of n for the results of the present study are discussed in Sect. 3.2.5. Aircraft-related BC particles can show different sizes and morphologies compared to BC related to surface sources. The treatment of aircraft-induced particles in the model is described below.

2.3. Aircraft BC emissions

Aircraft BC emissions are calculated here from the global aviation fuel consumption data provided by Schmitt and Brunner (1997) for aircraft activity as occurred in 1992. The data contains information on the global distribution of aircraft fuel use and its annual cycle. A detailed error analysis of global aviation fuel consumption scenarios (IPCC, 1999) reveals that the fuel consumption data used here accounts for only 73%

of the amount of aviation fuel produced in 1992. Hence, aviation fuel consumption may be underrepresented in the present study by up to 20–30%. According to the annual growth rate of aviation fuel consumption (about 4% per year in the 1984 to 1992 period; IPCC, 1999), the aviation fuel use has increased by about 30% from the mid-1980s to 1992. Hence, an underestimation as described above would make the aviation fuel consumption data highly conformable with the BC surface emissions which are representative of the mid-1980s.

BC emission rates are derived from the aircraft fuel consumption data using BC emission indices (EIs) typical of commercial aircraft operating in 1992. Emission indices for BC mass emission rates, EI(M), have been provided by Döpelheuer (1997) and Petzold et al. (1999). An update of these EIs including an altitudinal variation is used here. Representative EIs were determined for different altitudinal ranges considering variations in engine type and power conditions (Döpelheuer, 2002). As shown in Fig. 1, the EI(M) decreases from values in the range of 0.08 g(BC)/kg(fuel) at the lowest flight levels to values around 0.02 g(BC)/kg(fuel) at 11.5 km and increases again to 0.08 g(BC)/kg(fuel) at 16 km to account for supersonic aircraft. The 1992 fleet average EI(M) amounts to 0.038 g(BC)/kg(fuel). To derive the number concentration of BC particles resulting from aviation, aircraft exhaust BC number-to-mass ratios also representative of the 1992 fleet are employed (Döpelheuer, 2002). The number-to-mass ratios, also referred to as particle number EIs or EI(N), range from 4.8×10^{15} particles/g(BC) at the surface to around 1.6×10^{16} particles/g(BC) at cruise altitude (Fig. 1). Note, that these values exceed the number-to-mass ratio assumed for particles related to surface sources (Sect. 2.2) by an order of magnitude (factor 22 at cruise altitude, factor 7 at surface).

Annual mean vertically integrated BC emissions due to aviation, derived from the aviation fuel consumption data and the EIs described above, are displayed in Fig. 2. The figure reveals that the major fraction of the aircraft BC emissions occur at northern midlatitudes, especially over North America, the North Atlantic, and Europe. The vertical distribution of the BC emission rates considered (not shown) reveals that 38% by

mass and 58% by number of the total aircraft BC emissions occur at the main flight levels between 10 km and 12 km altitude. The seasonal variation considered (not shown) can be large in remote areas but is only small in the main flight regions (mostly within 10%). The total global emission rate of BC from aviation amounts to 0.0047 TgC yr^{-1}.

2.4. Aircraft BC mass and number concentrations

To quantify the aircraft contribution to the total BC burden in our simulations, aircraft related BC is numerically represented as an individual trace constituent treated separately from BC originating from surface sources. It is likely that aircraft-generated BC particles become hydrophilic due to activation by chemical processing or deposition of H_2O and water soluble material in contrails and perhaps also in plumes that do not form contrails (Kärcher, 1999). Hence aircraft-induced BC is generally assumed to be hydrophilic in the present study. The mass cycle of BC from aircraft is simulated as described in Sect. 2.2 for hydrophilic BC. The particle number concentration of aviation-induced BC is treated differently from that of BC particles originating from surface sources. This will be described in the following.

As mentioned in Sect. 2.2, the number concentration of BC particles from surface sources is derived from the mass concentration assuming a constant number-to-mass ratio. This appears to be justified since BC from surface sources can probably be regarded as aged aerosol in the UTLS characterized by a quasi-invariant size distribution. However, BC from aircraft may possess highly variable number-to-mass ratios ranging from those which are characteristic of fresh exhaust (Sect. 2.3) to smaller number-to-mass ratios typical of aged particles. The latter may show a larger degree of agglomeration and may also be mixed with BC emitted at the surface or with other particulate matter not generated by aircraft. As discussed in the Appendix, the main processes which potentially reduce the number-to-mass ratio of aircraft-related BC particles are the scavenging of aviation BC by larger liquid background aerosols and the scavenging by cloud particles. It is currently not well understood how immersed BC particles are processed within aerosols or cloud particles. Many effects of this processing are con-

ACPD
4, 3485–3533, 2004

ceivable, but observational confirmation for such processes is lacking. Regarding these uncertainties, the number-to-mass ratio of "aged" BC from aviation is not included in the simulations presented here. This implies that the aviation-induced perturbation of the BC particle number concentration cannot be quantified in detail. However, it still can be delimited by maximum and minimum estimates.

To achieve this, BC from aviation is subdivided into "fresh" and "aged" BC. "Fresh" BC is generated according to the BC emission rate. The transformation of "fresh" to "aged" particles is parameterized considering the major ageing processes which potentially reduce the number-to-mass ratio. For a detailed description of this parameterization, we refer to the Appendix. Considering a very efficient particle ageing results in a minimum estimate $M_{f,min}$ of the amount of "fresh" BC from aviation. As shown in the Appendix, it is very likely that the amount $M_{f,min}$ of aircraft-generated BC retains the particle number-to-mass ratio EI(N) typical of the fresh exhaust (Sect. 2.3). Therefore, a minimum estimate N_{min} of the number concentration of aviation-induced BC particles can be derived from $M_{f,min}$ as:

$$N_{min} = EI(N) \times M_{f,min} \tag{1}$$

A corresponding maximum estimate can be provided by assuming that the number-to-mass ratio is not affected by particle ageing. In this case, the number-to-mass ratio EI(N) applies to the total amount of BC from aviation which can be calculated from the sum of $M_{f,min}$ and the complementary amount $M_{a,max}$ of aged BC:

$$N_{max} = EI(N) \times (M_{f,min} + M_{a,max}) \tag{2}$$

The mass concentration M of BC from aircraft can be influenced by BC emissions occurring at different locations. Therefore, local application of Eqs. (1) and (2) requires a constant EI(N). In our simulations, EI(N) varies with altitude and BC from aviation can experience vertical transport and mixing. To overcome this problem, the aviation impact is delimited by solving prognostic equations for $M_{f,min}$, $M_{a,max}$, and the corresponding number concentrations $N_{f,min}$ and $N_{a,max}$. $N_{f,min}$ is equivalent to N_{min}.

ACPD
4, 3485–3533, 2004

$N_{a,max}$ is the number concentration of aged particles resulting from the assumption that the number-to-mass ratio is unaffected by particle ageing. $N_{a,max}$ has to be added to $N_{f,min}$ to obtain N_{max}. The production of $N_{f,min}$ is calculated from EI(N) and the aviation BC mass emission rate. Transport and removal of the number concentrations are simulated in analogy to BC mass (Sect. 2.2). Particle ageing is considered according to Eq. (A1)(Appendix).

3. Model studies

3.1. Description of the simulations

To assess the impact of aviation on the atmospheric BC budget, a set of model experiments (Table 1) was performed using the model framework described in Sect. 2. A simulation with the standard version of the model was performed which is taken as the reference simulation and which will be referred to as the "BASE" simulation.

The relative contribution of aircraft emissions to the BC budget of the UTLS depends on the corresponding contribution of BC from surface sources which currently is uncertain (Sect. 1). A key uncertainty in simulations of the atmospheric BC cycle is the efficiency of BC removal. Therefore, the atmospheric residence time of BC can be misrepresented which complicates the evaluation of BC fluxes from the surface to the UTLS. To investigate the impact of this uncertainty on the UTLS BC budget simulated here, two additional model experiments were performed assuming increased/decreased BC removal efficiencies. This was achieved as follows: BC is removed from the atmosphere by wet and dry deposition. The efficiency of the simulated BC wet deposition is strongly controlled by the hygroscopic properties of BC which currently are not well understood. In contrast to hydrophobic BC, hydrophilic BC can be scavenged by cloud droplets and ice particles. Therefore the wet deposition efficiency of BC depends on the ratio of hydrophilic to hydrophobic BC. The hygroscopic properties of BC also control its dry deposition efficiency, since hydrophilic BC is deposited more efficiently over

wetted surfaces. Hence, the simulated ratio of hydrophilic to hydrophobic BC is a key parameter controlling the efficiency of both wet and dry BC removal processes. In the BASE simulation, 80% of the BC emissions from surface sources are assumed as hydrophobic, 20% as hydrophilic (Sect. 2.2). With an e-folding time of 24 h, hydrophobic BC is assumed to become hydrophilic. In the first sensitivity experiment, BC particles are generally assumed to be hydrophilic (experiment "PHIL"). Consequently, BC is removed more efficiently compared to the BASE simulation. In a second sensitivity experiment, an e-folding time of 48 h is assumed for the conversion of hydrophobic into hydrophilic BC (experiment "PHOB"). Therefore BC is removed less efficiently compared to the BASE simulation.

In the global model study by Danilin et al. (1998) on the aviation impact on the UTLS BC load, the impact of wet removal was neglected above 400 hPa. In order to make the results of the present study more comparable to the previous study and in order to assess the impact of BC removal in high clouds, a third sensitivity experiment ("NOICE") was accomplished. Cloud water in the UTLS is mainly present in the ice phase. In the NOICE simulation, scavenging of BC by ice particles is neglected at pressure levels above 400 hPa. The NOICE simulation will be discussed in Sect. 3.2.4 where we compare our results to the simulations performed by Danilin et al. (1998).

The model experiments described above are based on simulations assuming a prescribed annual cycle of sea surface temperatures according to climatological values for the respective month. For each individual experiment, 4-year integrations were performed after a 15-month model spin-up. To provide a robust statistical base for the main conclusions, additional 6 model years were simulated for the BASE experiment. The prolonged (10-year) integration leads to very similar conclusions than the 4-year BASE simulation. The differences in the UTLS BC load occurring between the 4-year and the 10-year simulations are generally not larger than a few percent. There is no trend detectable in the UTLS. These statements hold for total BC and for aircraft-induced BC as well. Hence, with regard to the high computational expenses of the simulations, prolonged integrations were not performed for the PHIL, PHOB and NOICE experiments.

3.2. Results and discussion

3.2.1. Global distribution of UTLS BC mass loading

Global distributions of the total BC mass concentration simulated for the 250 hPa pressure level are shown in Fig. 3. The 250 hPa level is chosen since it is located within the main aircraft flight levels. The figure shows results obtained for winter and summer conditions in the BASE, the PHIL and the PHOB experiments.

The BC concentrations simulated in the BASE simulation for 250 hPa range between about 0.5 and 10 ng/m^3. The BC concentration fields at that pressure level clearly reflect the spatial and temporal variability of the BC surface sources described, for instance, by Liousse et al. (1996) and Cooke and Wilson (1996). As it will be shown in Sect. 3.2.4, the UTLS BC mass budget simulated here is dominated by BC originating from the surface.

The southern hemispheric BC sources are dominated by biomass burning. Due to the strong temporal and spatial variability of biomass burning events, also the BC concentrations simulated for 250 hPa in the southern hemisphere are characterized by a strong spatial and seasonal variability. At several locations, the southern hemispheric BC fields simulated for spring and autumn conditions (not shown) are very different from the BC fields obtained for the winter and summer seasons.

The BC emissions in the northern hemisphere, especially in the extratropics, are dominated by fossil fuel combustion. The major emission regions of BC from fossil fuel combustion are North America, Europe, and Southeast Asia. Due to upward transport of BC from the boundary layer, the plumes of these emission regions can clearly be identified at 250 hPa showing a significant spatial shift induced by westerly flows. Since the seasonal variation of the fossil fuel combustion source is small (such variation is not considered here for surface sources), these plumes are the persistent features in the northern midlatitude BC concentration field at 250 hPa at all seasons. The corresponding concentrations are highest during summer and lowest during winter which can be attributed to the seasonal cycle in vertical transport efficiency.

ACPD
4, 3485–3533, 2004

As in previous global model studies (e.g. Cooke and Wilson, 1996; Cooke et al., 2002), the results obtained in the PHIL and PHOB experiments reveal that the BC concentrations simulated for the UTLS show a marked sensitivity to the prescribed hygroscopic properties of BC. When BC is totally hydrophilic (case PHIL), the simulated UTLS BC concentrations are significantly smaller compared to the BASE case. If a larger fraction of BC is hydrophobic (case PHOB), the UTLS BC concentration increases by factors around 2 compared to the reference experiment. These differences are also reflected in the total atmospheric BC burden which, on average, amounts to 0.213, 0.174 and 0.244 TgC in the BASE, PHIL and PHOB simulations, respectively.

3.2.2. Comparison to observations

The sensitivity experiments described above were performed since the current knowledge about BC hygroscopicity and BC-cloud interactions is poor. To evaluate which of the experiments is most realistic with regard to UTLS BC, the model results have to be compared to observations. Some data sets are available focusing on BC concentrations in aircraft plumes (e.g. Petzold et al., 1999). Due to the small spatial scales of the plumes, these data cannot be used for evaluating large-scale model output. Only a few data sets of UTLS BC measurements not taken in young aircraft plumes are currently available (Pueschel et al., 1992; Blake and Kato, 1995; Baumgardner et al., 2003, 2004). These measurements were carried out at a large variety of locations during different episodes. Nevertheless, from a climatological point of view, this data base is too sparse to perform a robust model evaluation. However, given the lack of additional data, we used the measurements to obtain a first guess of the model quality. Additional observations of BC in the UTLS are needed to consolidate the model evaluation.

Figure 4 shows BC concentrations simulated in the BASE, PHIL and PHOB experiments in comparison to the observational data documented by Blake and Kato (1995) (BK95). This data set includes BC concentrations measured from aircraft in the UTLS during different field campaigns at various locations. Parts of the data were already

described by Pueschel et al. (1992). For the comparison, we considered the BC concentrations of the data points located between 5 and 15 km altitude as well as the corresponding uncertainties (data taken from Table 1 in BK95 and adjusted from standard to ambient conditions). The analysis method used by BK95 to derive BC concentrations from wire impactor samples didn't take into account the fractal shape of BC particles and didn't account for particle bounce. Strawa et al. (1999) showed with a modified method that these simplifications lead to an underestimation of the BC concentration by a factor of 6 on average. Furthermore, Blake and Kato (1995) stressed that small BC particles tend to be underrepresented in the wire impactor samples. Black carbon particles immersed within larger spherical liquid aerosols are generally not detected by the BK95 and the Strawa et al. (1999) method. These uncertainties have to be carefully considered when simulated BC concentrations are compared to the BK95 data. The uncertainties provided by BK95 (Table 1 in BK95) which are shown in Fig. 4 are probably too low.

The simulated BC concentrations plotted in Fig. 4 were extracted from the model output for the locations, altitudes, and months of the respective measurements. Since the simulated BC concentrations show an asymmetric frequency distribution (frequency maximum shifted towards small concentrations), median concentrations are analyzed here rather than averages. The median values as well as the corresponding standard deviations displayed in Fig. 4 were derived from 12-hourly averaged model output assuming a lognormal frequency distribution of the BC concentrations. The resulting concentrations are more representative for the values typically occurring in the simulations than the corresponding averages.

Figure 4 also shows comparisons of the simulations to the recent aircraft measurements of light absorbing particles (LAP) performed by Baumgardner et al. (2003, 2004) (BEA03) in the UTLS over the North Atlantic and the Arctic Sea during a winter episode in 2003. A newly developed single particle soot photometer was applied for these measurements. The uncertainty of this method is reported as ±50%. The lower detection particle size limit is 0.15 μm. The technical details are described by Baumgardner

et al. (2003, 2004) and Stephens et al. (2003). The major fraction of the observed LAP particles was found to be BC. However, a large fraction (>40%) was found to be non-BC particles mainly composed of metals. For comparing the data to the simulations, the measured data was averaged over flight segments defined by projecting the flight tracks on the model grid. In analogy to the analysis of the simulations, median LAP concentrations and corresponding standard deviations are then derived from these averages. Therefore, the data was subsumed for the areas between 60° N and 70° N and north of 70° N, respectively. Only those measurements taken above 5 km (all measurements were taken below 15 km) were considered. Differences of the resulting BC concentrations shown in Fig. 4 to the values presented by Baumgardner et al. (2004) are due to the use of median concentrations instead of averages and due to the inclusion of data taken in the upper troposphere.

Given the large uncertainties of the BK95 data, a detailed quantitative comparison of these data to the simulations would be not reasonable. Nevertheless, some qualitative features can be compared. The spatial variation of the BC concentrations simulated in the BASE case is similar to that observed by BK95. Both the measurements and the simulations show a marked contrast between polluted continental and remote marine air masses. The smallest BC concentrations occur over the central Pacific whereas large concentrations are found over eastern North America. The data points over western North America, where continental and marine influences compete, tend to show medium concentrations in the BK95 data as well as in the simulation. This is also the case for the northern high latitude data. Nevertheless, the differences in the BC concentration occurring between polluted continental and remote areas are more pronounced in the measurements. This possibly reflects that BC immersed within larger liquid aerosol is underrepresented in the BK95 data. Black carbon occurring in remote areas may have been transported over long distances. This implies a large probability that a significant fraction of this BC has been immersed and, therefore, is not detected with the BK95 method.

The BC concentrations simulated in the BASE experiment are well accordable with

the BEA03 data taken north of 70° N. Taking into account that about 50% of the LAP is BC, the simulated and observed median BC concentrations nearly match. Between 60° N and 70° N, the simulated BC concentrations are similar to the LAP concentrations observed by BEA03. However, the simulated concentrations exceed the observed values after taking into account that only about 50% of the observed LAP is BC. Nevertheless, within the given variability ranges, the simulations are accordable with the measured values. Observations performed by Neusüß et al. (2000a,b, 2002) and Matta et al. (2003) under a variety of conditions indicate that the BC mass contained in particles smaller than 0.15 μm mostly is small. The contribution of these particles to total BC was generally below 30% during the measurements. Hence, the absence of small particles in the observations appears to be of secondary importance for the comparison.

The BC concentrations simulated in the PHIL and PHOB experiments which are also displayed in Fig. 4 show spatial variations quite similar to those simulated in the BASE case. However, the simulated absolute BC loadings show marked differences to the BASE experiment. As already discussed in Sect. 3.2.1, the PHIL and PHOB simulations tend to show smaller and larger concentrations, respectively. When we consider that about 50% of the LAP is BC, the PHIL experiment is well accordable with the BEA03 measurements taken between 60° N and 70° N but shows too small concentrations north of 70° N. Under the same assumption, the PHOB simulation shows too much BC. Hence the BASE simulation appears to be most conformable with the BEA03 data. Given the large uncertainty of the BK95 data, we focus on the BASE case in the assessment of the aviation impact (Sects. 3.2.4 and 3.2.5).

3.2.3. Comparison to other global model studies

Comparisons of BC simulations with the observational data by Blake and Kato (1995) have also been performed in other global model studies (Cooke et al., 1999, 2002; Koch, 2001). As in the simulations performed here, the BC concentrations simulated by Cooke et al. (2002) and Koch (2001) show a similar spatial variation as observed by

Blake and Kato (1995). Cooke et al. (1999) focused on altitudinal variations and didn't analyse the geographical dependence. Due to the large uncertainties inherent in the measurements, the quality of the UTLS BC concentrations simulated by the different models cannot be evaluated here. Nevertheless, it is worthwhile to compare the UTLS BC concentrations obtained with different global model systems.

As mentioned in Sect. 1, simulations of the UTLS BC load are discussed in a couple of global model studies (Cooke and Wilson, 1996; Liousse et al., 1996; Cooke et al., 1999, 2002; Koch, 2001; Köhler et al., 2001; Chung and Seinfeld, 2002). The UTLS BC concentrations obtained with the different model approaches can show significant deviations. The zonal mean BC concentrations simulated for the pressure range between 300 and 200 hPa in the northern hemisphere vary from values of 1–10 ng/m^3 (Liousse et al., 1996, and this study) to values of 10–50 ng/m^3 (Cooke and Wilson, 1996; Koch, 2001). The studies by Chung and Seinfeld (2002), Cooke et al. (1999, 2002) and Köhler et al. (2001) show intermediate concentrations. The corresponding BC concentrations in the southern hemisphere are typically an order of magnitude smaller but mostly show similar differences between the various model approaches.

The discrepancies can have manifold reasons. The studies of Cooke et al. (1999) and Cooke et al. (2002) take into account BC emissions from fossil fuel combustion only which causes marked differences to the other studies especially in the tropics and the southern hemisphere where biomass burning is the dominating BC source. The simulations by Cooke et al. show comparatively small BC concentrations in the southern hemispheric UTLS. The other studies include BC from both biomass burning and fossil fuel combustion. Since the total emission rates vary only slightly between these studies, differences in the emission scenarios probably are of secondary importance for the simulated UTLS BC budget. Sensitivity experiments performed in some of the studies demonstrate that the simulated UTLS BC concentrations are very sensitive to the treatment of BC wet removal (see also Sect. 3.2.1). Hence, parts of the deviations described above can probably be attributed to different representations of the BC hygroscopicity, precipitation scavenging or precipitation itself. The studies by Danilin et al.

(1998) and Rogers et al. (2002), where aircraft emission tracer simulations performed with a large set of global models were compared, indicate that also differences in the transport characteristics of the models can be very important (see also Sect. 3.2.4).

Due to the lack of extensive observations of BC in the UTLS, it is currently not possible to evaluate the quality of the simulations discussed above. Given the distinct differences in UTLS BC simulated with the different models, absolute contributions of different sources to the atmospheric BC cycle are not necessarily comparable if they were estimated with different models. This implies that a quantitative investigation of the relative impact of aircraft emissions to the atmospheric BC budget should be based on a consistent model approach including all relevant BC sources. Most of the studies discussed above didn't take into account BC emissions from aviation. However, large UTLS BC concentrations were simulated neglecting the aviation impact. This clearly demonstrates that the contribution of surface sources to the UTLS BC budget can be large in simulations of UTLS BC. This further implies that estimates of the relative aviation impact based on comparisons of simulations including only the aviation source (Danilin et al., 1998; Rahmes et al., 1998) with BC observations are not reasonable. In the present study, simulations including both BC from aviation and from surface sources are performed. Estimates of the absolute and relative aviation impacts based on these simulations are discussed below.

3.2.4. Contribution of aviation to BC mass loading

Figure 5 highlights the absolute and relative contribution of BC from aviation to the BC mass concentration at 250 hPa (main flight level) as simulated in the BASE case for winter and summer conditions. The amount of BC resulting from aviation is largest at northern midlatitudes. Maximum contributions of more than 0.05 ng/m^3 occur in the main flight areas over North America, the North Atlantic and Europe. The aviation contribution at 250 hPa generally exceeds 0.02 ng/m^3 at northern midlatitudes and decreases strongly from the northern to the southern hemisphere. The absolute aviation impact is largest during summer when the vertical inflow from lower layers car-

rying higher amounts of aircraft BC (Fig. 6) is largest. Note that the aircraft-induced BC perturbations simulated for spring and autumn conditions (not shown) exhibit no extraordinary features and fit smoothly in the annual cycle suggested by the results obtained for winter and summer.

Compared to the total BC mass concentrations present at 250 hPa (Fig. 3), the contribution from aircraft is small. Maximum relative contributions of 2–3% during winter and 1–2% during summer are simulated. The aviation-induced perturbations of UTLS BC are clearly smaller than the inter-annual variability of the mass concentration of northern hemispheric UTLS BC originating from the surface (standard deviations of around 0.1–1 ng/m^3 in the 10-year BASE simulation). Hence, the simulations reveal that the contribution of aviation to the UTLS BC mass budget is of limited importance. This result is similar to the findings of the model study by Kjellström et al. (1999) for aviation sulfur emissions. Kjellström et al. (1999) demonstrated that the fraction of the UTLS sulfate mass loading resulting from air traffic typical of 1991/1992 probably is very small, even in the most frequented flight regions (<1% north of 40° N).

Vertical distributions of zonal mean total and aviation-induced BC mass concentration are displayed in Fig. 6. The zonal means of the simulated total BC mass concentrations range from more than 100 ng/m^3 in the boundary layer at low latitudes and northern midlatitudes to values on the order of 1 ng/m^3 in the UTLS and the lower and middle troposphere at southern mid- and high latitudes. A distinct seasonal cycle of UTLS BC is simulated for the northern midlatitudes showing the largest concentrations during summer when convective upward transport from the boundary layer is most efficient. The contribution of BC from aviation is largest at northern midlatitudes where the zonal mean aviation contribution ranges from up to 0.1 ng/m^3 in the lower troposphere to values around 0.01–0.05 ng/m^3 in the UTLS. The vertical distributions reveal that the relative aircraft-induced BC perturbation is largest in the UTLS. Despite that mass concentrations of BC from aircraft are largest in the lower troposphere, the aviation-induced perturbation is very small compared to the large lower tropospheric BC loading resulting from other sources.

ACPD
4, 3485–3533, 2004

Annual averages of the zonal mean aircraft-induced BC perturbations simulated in the BASE and the NOICE experiments are presented in Figs. 7b and d. The BASE experiment shows distinct differences to the corresponding results of the previous studies by Danilin et al. (1998) and Rahmes et al. (1998)(see also Sect. 1). In the BASE experiment, the aviation-induced BC perturbations amount to 0.02–0.05 ng/m^3 in the northern hemispheric UTLS. The corresponding BC perturbations obtained with a previous version of the ECHAM GCM in the study by Danilin et al. (1998) assuming a constant emission index of 0.04 g(BC)/kg(fuel) range between 0.05 and 0.2 ng/m^3. The smaller values obtained in the present study are mainly attributed to changes in the BC emission indices as well as the different representation of BC removal. In the present study, the emissions index decreases from 0.08 g(BC)/kg(fuel) at the surface to values between 0.02 and 0.03 g(BC)/kg(fuel) in the main flight altitudes (Sect. 2.3; Fig. 1). Since the aviation fuel consumption assumed by Danilin et al. (1998) is similar to that assumed here, the differences in the BC emission indices lead to less efficient UTLS BC emissions in the present study. In contrast to the BASE simulation performed here, BC removal by precipitation was neglected by Danilin et al. (1998) above the 400 hPa level. At these altitudes, precipitation occurs mainly due to the sedimentation of ice crystals. The NOICE simulation demonstrates that neglecting the scavenging of BC by ice increases the aviation-induced BC perturbation by more than a factor of 2 (Figs. 7b and d).

Hence the adoption of updated emission indices as well as the inclusion of in-situ BC removal by precipitation largely explain the differences in the aviation-induced BC perturbations occurring between the BASE experiment and the ECHAM simulation discussed by Danilin et al. (1998). Differences in the transport characteristics of ECHAM version 3 used by Danilin et al. (1998) and ECHAM version 4 which was employed here appear to be of secondary importance for the dispersion of subsonic aricraft emissions (Rogers et al., 2002).

The maximum fuel tracer concentrations simulated by Danilin et al. (1998), which were generally obtained in the main flight levels, vary by a factor of 10 between the

different model approaches. Nevertheless, the variation stays within a factor of 2 when the fuel tracer amount is integrated over the northern hemispheric UTLS. The variation further decreases to less than 1.5 when the results of the 2-D models are not taken into account. This reflects that large local differences can occur between the different simulations but that the large-scale features of the simulated aviation fuel tracer distributions are similar, especially in the 3-D simulations. Hence, differences between the large-scale features of the aircraft-induced perturbation simulated in the BASE experiment and the perturbations obtained by the models applied by Danilin et al. (1998) can, to a large extend, be explained by the different assumptions on the BC emission index and BC removal. The differences in the maximum BC values, which are clearly larger, also result from the different transport characteristics of the respective models. The largest differences in the maximum perturbations simulated here and in the Danilin et al. (1998) study occur when the results of some of the 2-D models are considered. Compared to most of the 3-D simulations, these models suggest extraordinary high maximum aircraft-induced BC concentrations. Also the maximum value of the BC perturbation simulated in the 2-D model study by Rahmes et al. (1998) is in the upper range of the simulated values.

It can be concluded that the consideration of updated BC emission indices as well as the inclusion of precipitation scavenging of BC within ice clouds reduces the aircraft-induced UTLS BC perturbations obtained in the present simulation for the northern hemispheric UTLS by factors of about 2–5. Without these changes, the simulations are consistent with previous simulations (Danilin et al., 1998).

The scavenging efficiency of BC by ice crystals is still debated. Hence also the scavenging efficiency assumed in the present study for hydrophylic BC (Sect. 2.2) is uncertain. Nevertheless, the measurements by Ström and Ohlsson (1998) suggest that significant amounts of BC from aircraft are incorporated into ice crystals and, therefore, can be removed from the UTLS via ice sedimentation. The results shown in Fig. 7 demonstrate that varying the assumptions on the removal efficiency of BC by ice sedimentation has a similar effect on the concentrations of BC from aircraft and from

surface sources. Hence, the relative contribution of aviation to the UTLS BC budget simulated here appears to be not very sensitive to the assumptions on BC removal in ice clouds. The absolute contribution, however, can be destinctively smaller than suggested by previous studies.

3.2.5. BC particle number concentration

Given the small aircraft-related perturbations of the BC mass concentration simulated here, the question should be addressed whether a larger perturbation of the BC particle number concentration can be expected. Figure 8 highlights the BC particle number concentrations simulated for the 250 hPa level in the BASE experiment for winter and summer conditions. The spatial variation in number concentration of BC particles from surface sources (Figs. 8a and b) is very similar to the corresponding variation of total BC mass concentration (Figs. 3a and b). This is due to the constant number-to-mass ratio assumed for BC originating from the surface (Sect. 2.2). The number concentration of surface-related BC particles simulated for 250 hPa typically ranges between 0.2 and 10 cm^{-3} and generally exceeds 1 cm^{-3} at northern midlatitudes.

Number concentrations of aircraft-induced BC particles simulated for 250 hPa are highlighted in Figs. 8c–f. When the large number-to-mass ratios typical of fresh aircraft exhaust BC (Sect. 2.3) are generally considered for BC from aircraft, a maximum potential contribution of aviation to the number concentration of UTLS BC particles can be estimated (Sect. 2.4). As displayed in Figs. 8c and d, these maximum estimated particle number concentrations range between about 0.2 and 1 cm^{-3} and mostly exceed 0.5 cm^{-3} in the most frequented flight regions over North America, the North Atlantic, and Europe.

Relating these maximum estimates for the number concentration of BC from aviation to the number concentrations obtained for surface-related BC particles, a maximum estimate for the relative contribution of BC from aviation to the total BC number concentration can be provided. During winter (Fig. 9a), the maximum estimated aviation contribution amounts to more than 20% over large parts of the northern hemisphere.

ACPD
4, 3485–3533, 2004

The largest contributions range up to 40% and are simulated for the main flight areas. Even during summer (Fig. 9b), when the background BC burden is largest, maximum estimated contributions of 10–30% are obtained for the northern hemisphere. As in the case of the BC mass concentrations, the perturbations simulated for spring and autumn (not shown) fit smoothly into the seasonal cycle suggested above. In large parts of the most frequented flight areas, the maximum estimated aircraft-induced perturbations are larger than the inter-annual variability of the number concentration of surface-related BC particles (standard deviations of around 0.1–1 particles/cm^3 in the 10-year BASE simulation). Hence, the simulations indicate a high potential of aviation to induce significant increases in the UTLS BC particle number concentration. If BC particles from aircraft can serve as heterogeneous ice nuclei, this might have important implications for the formation of cirrus clouds (e.g. Jensen and Toon, 1997; Kärcher and Lohmann, 2003).

The number-to-mass ratios of BC particles inherent in fresh aircraft exhaust are large owing to the comparably small sizes of the emitted BC particles of ≈20–40 nm (e.g. Petzold et al., 1999; Döpelheuer, 2002). In contrast to BC from surface sources which we assume as aged particles characterized by a constant number-to-mass ratio, BC from aviation is emitted directly into the UTLS. Hence, in-situ ageing processes of the fresh aircraft exhaust and related decreases in the exhaust BC particle number-to-mass ratio may be very relevant for quantifying the impact of aviation on UTLS BC particle number concentration (see also, Sect. 2.4). The question is whether such ageing processes may lead to a strong reduction of the maximum estimated aircraft-induced BC particle number perturbations described above.

A minimum estimate of the number concentration of BC from aircraft was performed considering the major ageing processes and assuming the ageing to be very efficient (see Sect. 2.4 and the Appendix). The results presented in Figs. 8e, f, 9c, and d reveal that even this minimum particle number concentration would make a relevant contribution to the total UTLS BC particle number concentration. The minimum estimated aircraft contribution at 250 hPa frequently exceeds 10% in the northern hemisphere

ACPD
4, 3485–3533, 2004

and amounts up to 20% in the main frequented flight areas.

Corresponding to the results shown in Fig. 8, vertical distributions of the zonal mean particle number concentration of BC emitted at the surface as well as of BC resulting from aviation are displayed in Fig. 10. As in the case of mass concentration, the vertical distributions indicate that the relative aircraft-induced perturbation of the BC particle number concentration is largest in the UTLS. In the lower and middle troposphere, the aviation-induced contribution is small compared to the large numbers of BC particles originating from the surface.

In comparing the estimates of number concentrations of BC particles originating from aviation and from surface sources, we recall that a constant number-to-mass ratio is assumed for BC particles originating from the surface. As described in Sect. 2.2, this number-to-mass ratio is derived from the assumption that the surface-related BC particles contain n=10 spherically shaped primary particles on average. The morphologies of BC particles collected in the tropopause region (Blake and Kato, 1995; Pueschel et al., 2000) and the lower stratosphere (Strawa et al., 1999) reveal that much larger agglomerates can reside at these altitudes. Hence, the average n may be larger than assumed. If these large BC particles mainly originate from surface sources, the number concentrations of the surface-related BC particles could be lower than simulated here. Consequently, the relative impact of aviation on the UTLS BC particle number would be larger than estimated above. However, it is not clear whether the BC morphologies supplied by the limited number of measurements are representative of UTLS BC. Furthermore, the origin (aviation or surface) of the observed BC particles is not known. Due to a lack of observational data on the UTLS BC particle number concentration, a validation of the simulated BC particle numbers is currently impossible.

4. Conclusions

Simulations with the ECHAM4 GCM were performed to assess the global BC budget. The special focus was to quantify the impact of aviation on the global UTLS BC mass

and particle number loading. The main findings resulting from these simulations are:

1. The BC mass concentrations simulated for the UTLS typically range between 0.1 and 10 ng/m^3 and generally exceed 1 ng/m^3 in the northern midaltitude UTLS. A good agreement with recent observational data on UTLS BC mass loading taken over the North Atlantic and the Arctic Sea (Baumgardner et al., 2003, 2004) was found. The model is capable of reproducing the spatial variation of UTLS BC concentrations observed at different locations of the globe in earlier measurements by Blake and Kato (1995). Nevertheless, the large uncertainty of these measurements hampers a detailed evaluation of the model quality.

2. The UTLS BC mass loading induced by aircraft typically ranges between 0.01 and 0.1 ng/m^3 at northern midlatitudes where the aviation impact is largest. Hence the contribution of aircraft to the total BC mass loading simulated here for the UTLS is small. The relative large-scale contribution does not exceed a few percent, even in areas highly frequented by aircraft.

3. The number concentrations of BC particles derived from the UTLS BC mass loading originating from surface sources typically range between 0.1 and 10 cm^{-3} and frequently exceed 1 cm^{-3} at northern midlatitudes. Observational data suitable to perform a validation of the simulated UTLS BC particle number concentrations are urgently required.

4. The simulations suggest that the perturbations in UTLS BC particle number concentrations resulting from aircraft are larger than the corresponding perturbations of the BC mass loading, mainly caused by the small sizes of aircraft-generated BC particles. Large-scale number concentrations of UTLS BC resulting from aircraft of more than 0.5 cm^{-3} are simulated for the main flight areas when BC particle number-to-mass ratios typical of fresh aircraft exhaust are considered. This corresponds to an aviation contribution to the total BC particle number concentration ranging between 10 and 40%. Even when an efficient ageing of the aircraft particle exhaust is taken into account which leads to a reduction of the BC particle

number-to-mass ratio, the aviation contribution still amounts to 10–20% in the main flight areas. Hence the simulations indicate a large potential of aviation to induce significant perturbations in UTLS BC particle number concentration.

5. Large-scale impacts of aviation on the BC mass and particle number concentrations are very small in the lower troposphere.

In the light of these findings, we evaluate the potential climatic impacts of BC emissions from aviation as follows:

Direct climatic impacts: A first estimate of the direct impact of BC from aviation on the atmospheric radiation budget was provided by IPCC (1999). The direct radiative forcing attributed to the aviation-induced BC increase was estimated to be very small. A global mean forcing of only +0.003 (+0.001 to +0.006) W/m^2 was calculated considering the emissions of the 1992 fleet. The aviation-induced BC perturbation assumed in these calculations was significantly larger than the BC increase simulated in the present study. Hence, we suggest that the direct impact of BC from aviation could be even smaller than the IPCC (1999) estimates.

Indirect climatic impacts: It is currently debated whether BC from aviation may perturb the frequency or the microphysical and optical properties of cirrus clouds via heterogeneous ice nucleation on aviation-induced BC particles. The simulations performed here confirm that aviation has the potential to increase the atmospheric abundance of heterogeneous ice nuclei, provided that BC plays an important role in cirrus cloud formation and that ice can nucleate efficiently on BC particles from aircraft. The number concentrations of BC particles from aviation simulated here are large enough to cause significant changes in cirrus ice crystal number concentration and related changes in cirrus optical properties (Gierens, 2003; Haag et al., 2003; Kärcher and Lohmann, 2003). Therefore, more detailed knowledge about the role of heterogeneous nucleation in cirrus cloud formation as well as about the ice nucleating efficiency of different BC types and other atmospheric aerosols should be gained in the future. Regarding the rapid growth rates of aviation fuel consumption projected for the future

ACPD
4, 3485–3533, 2004

(3% per year until 2015 IPCC, 1999), the potential indirect impact of BC from aviation may become of increasing future importance. Hence, detailed future studies should focus on indirect climatic impacts of BC from aircraft.

The present study further reveals some important requirements for future refinements in global atmospheric BC simulations: i) The BC loading simulated for the UTLS strongly depends on the cloud scavenging efficiency of BC. The knowledge about the hygroscopic properties of atmospheric BC particles currently is very sparse. Hence extensive laboratory and field measurements of BC hygroscopicity are seriously required to increase the quality of future simulations of atmospheric BC. ii) As suggested by the aviation impact simulated here, anthropogenic perturbations of the atmospheric BC particle number concentrations can be very different from the corresponding perturbations of the BC mass loading. Therefore atmospheric aerosol models generally should include explicit predictions of aerosol particle number concentrations, rather than employing prescribed aerosol size distributions. iii) There is a lack of observations of the UTLS BC particle mass and number concentration. Much more of such observational data are urgently required to perform an adequate validation of global aerosol models.

Appendix: Ageing of aircraft exhaust BC

During the dispersion of aircraft exhaust from the young plume to spatial scales comparable to the grid resolution of large-scale models, the number concentration of the exhaust particles is reduced not only due to plume dilution but also due to scavenging of emitted particles by background aerosols or self-coagulation of exhaust particles. The plume dilution is implicitly considered here due to averaging the exhaust mass concentration over the respective large-scale model grid box. However, the reduction of particle number due to aerosol dynamical effects like coagulation is not a priori included.

To provide an estimate of the aerosol coagulation impact on the aircraft-induced perturbations of the BC particle number concentration, a parameterization of exhaust

particle ageing developed by Kärcher and Meilinger (1998) is employed. According to Kärcher and Meilinger, the dominant aerosol-aerosol interaction leading to changed particle number concentrations of the aircraft-induced BC population is the scavenging of BC particles by larger liquid background aerosols, a process which is still relevant after dispersion to large scales and which results in liquid particles showing BC immersions. A reduction of the total number concentration of particles containing aircraft BC occurs when more than one BC particle from aircraft is immersed in the same background particle. The number of fresh aircraft BC particles (not scavenged by larger aerosols) is estimated as (Kärcher and Meilinger, 1998):

$$N_f(t + \Delta t) = N_f(t) \times \exp[-K_{s,b} N_l(t) \Delta t]. \quad \text{(A1)}$$

Here $N_f(t)$ and $N_l(t)$ are the number concentrations of freshly aircraft-generated BC particles and the scavenging background particles, respectively, $K_{s,b}$ is a coagulation coefficient, here assumed to be $10^{-8}\,\mathrm{cm}^3\,\mathrm{s}^{-1}$ based on the particle sizes of aircraft-generated BC and background aerosols (see below), and Δt is the model time step. The model distinguishes between "fresh" and "aged" BC from aviation. Fresh BC (not scavenged by larger particles) is transformed into aged BC according to Eq. (A1). It is assumed that the mass transformation rate scales with the rate of number transformation. This assumption is justified since the size distribution of aircraft-generated BC is dominated by particles in a comparatively small size range (e.g. Petzold et al., 1999, and discussion below) and, therefore, impacts of particle size on the scavenging process are of secondary importance.

Size distributions characteristic of background aerosol particles in the free troposphere and the tropopause region at northern midlatitudes, where most of the aircraft emissions are released, are described by Schröder et al. (2002). Here we employ the size spectrum averaged for the two regimes which is bimodal lognormal with D_1=15 nm, D_2=88 nm, $\sigma_1=\sigma_2$=1.7 and which shows a particle number ratio of N_1/N_2=220/165. With these parameters the particle number concentrations present in the two modes can be derived from the background particle mass con-

centration predicted by the model. Typical aircraft-induced BC particle size spectra can be characterized as bimodal lognormal with number median diameters of D_1=30 nm and D_2=150 nm and corresponding geometric standard deviations of $\sigma_1=\sigma_2$=1.6 (Petzold et al., 1999). The number concentration is dominated strongly by the small particle mode. Hence, we neglect the large BC mode for calculating the scavenging rate. Since scavenging is more efficient for particles with different sizes than for particles showing comparable sizes, the interaction of the fine BC mode with large background particles can be expected to be more efficient than with fine background aerosols (comparable particle numbers in the two background particle modes). Therefore we only take into account the coagulation scavenging of the fine aircraft BC particles by large background aerosols. The number concentration of these particles $N_l(t)$ (Eq. A1) is identified with the number of the second mode sulfate and organic carbon particles which dominate the number concentration of background particles simulated for the UTLS.

In order to evaluate the quality of the simulated UTLS number concentrations of the larger background aerosols, comparisons with in-situ measurements were performed. Therefore, particle number concentrations observed during LACE 98 (Lindenberg Aerosol Characterization Experiment)(Petzold et al., 2002) and INCA (Interhemispheric differences in cirrus properties from anthropogenic emissions)(Minikin et al., 2003) were adopted. These data, which were gained from aircraft measurements taken in the troposphere and lowermost stratosphere under various conditions, provide information on the vertical distribution of the particle number concentration. Here, "accumulation mode" particle number concentrations obtained during the measurements by extracting particles with D_p>120 nm were compared to the corresponding fraction of the simulated N_l. A remarkably good agreement was found at pressure levels below 300 hPa. However, the observed number concentrations frequently exceed the simulated values above 300 hPa. At the 250 hPa level, for instance, which is located within the main flight levels, the deviation can reach factors around 3. It is not clear whether this is due to deficiencies in the particle number concentrations calculated from the simulated aerosol mass or due to extraordinary large UTLS number concentrations of

accumulation mode particles encountered during the respective measurements. Since the simulated UTLS sulfate loading is in good agreement with observations (Dibb et al., 1998, 2000), there seems to be no systematic underrepresentation of, at least, this major UTLS aerosol compound in the model. Nevertheless, deficiencies in the particle size distribution used to derive the particle numbers from aerosol mass or an underrepresentation of compounds other than sulfate can lead to too low particle number concentrations. In order to avoid an underestimation of the scavenging rate calculated from Eq. (A1), N_I was increased by a factor of 5 in the simulations performed here. Hence, the ageing of aircraft BC particles can be regarded as very efficient in the model. A potential underestimation of the scavenging rate due to the neglect of the BC interactions with smaller background particles or due to an underestimated coagulation coefficient may also be compensated by increasing the scavenging rate.

Ageing of aircraft-induced BC populations may also occur via cloud processing. BC particles from aircraft can be scavenged by cloud droplets or ice crystals. The BC particles can then be removed by precipitation or can be released by re-evaporation of clouds or precipitation. In the case of re-evaporation, the released aircraft BC particles could be incorporated within larger agglomerates of scavenged particles. Hence, cloud processing potentially results in a reduction of the aircraft BC particle number-to-mass ratio. In order to quantify the fraction of aircraft-induced particles which potentially has been processed in clouds, fresh aircraft BC particles are transformed into aged aircraft particles as soon as significant cloud activity occurs within the air mass carrying the BC particles. In the current model version the transformation is activated as soon as the cloud liquid water content and the cloud droplet number concentration exceed $5\,\mathrm{mg\,m^{-3}}$ and $10\,\mathrm{cm^{-3}}$ or as soon as the ice water content and the ice crystal number concentration exceed $0.5\,\mathrm{mg\,m^{-3}}$ and $0.1\,\mathrm{cm^{-3}}$. These values can be regarded as lower limit thresholds for the occurrence of significant cloud activity (e.g. Pruppacher and Klett, 1997). Hence, not only the BC processing by background aerosols but also the cloud processing of BC from aircraft is chosen to be very efficient in the model. Since the knowledge about aerosol-cloud interactions is currently too sparse to enable a detailed

ACPD
4, 3485–3533, 2004

assessment of the in-cloud processing of BC particles, we use the technique described above to identify the fraction of aircraft-generated BC which potentially interacted with cloud particles.

Aircraft exhaust BC can also interact with contrail ice. Exhaust BC particles can be incorporated into contrail ice by serving as heterogeneous ice nuclei or by coagulation scavenging by contrail ice particles (Kärcher, 1999). Incorporation during contrail formation substantially reduces the number concentration of the BC particles but is unlikely to cause persistent changes of their number-to-mass ratio in the case of short-lived contrails (Schröder et al., 1998). Loss of BC particles due to scavenging by contrail ice becomes relevant only in ageing, persistent contrails (Kärcher, 1999). Hence, only in the case of persistent contrails BC-ice interactions may cause significant reductions of the BC particle number-to-mass ratio. The magnitude of these changes has not yet been quantified by measurements. Persistent contrails form at or above ice saturation. Since the frequency of ice supersaturated regions mostly is smaller than 25% in the main flight areas (Gierens et al., 2000), the impact of contrail ice particles on BC from aviation is neglected here.

In summary, the techniques described above enable the separation between fresh and aged aviation-induced BC particles. Since the ageing processes are assumed to be very efficient, the simulated amount of fresh BC particles can be regarded as a minimum estimate. The aged particles potentially interacted with background aerosols or clouds. Since the details of these interactions are not well understood yet, the number concentration of the aged BC particles is not simulated here. Hence, the total number of particles containing BC from aviation is not quantified. However, as described in Sect. 2.4, the separation of fresh and aged BC is used to delimit the aircraft-induced perturbation of the BC particle number concentration.

Acknowledgements. We thank V. Grewe, A. Lauer and M. Ponater for helpful discussions of the ECHAM4 simulations. This research was supported by the “Helmholtz Gemeinschaft Deutscher Forschungszentren” (HGF) through the project “Particles and Cirrus Clouds” (PAZI). The U.S. Office of Naval research funded the development of the single particle soot photome-

ter (SP2) and the NASA Radiation Sciences Program funded the participation of the SP2 in the SOLVE II research program. The SP2 was developed by Droplet Measurement Technologies by G. Kok, who was also responsible for making the measurements during SOLVE.

References

Baumgardner, D., Kok, G., Raga, G., Diskin, G., and Sachse, G.: Black carbon measurements in the arctic UT/LS, Proceedings of the European Aerosol Conference 2003, J. Aerosol Sci., 979–980, 2003. 3487, 3488, 3498, 3499, 3510, 3527

Baumgardner, D., Kok, G., and Raga, G.: Warming of the arctic lower stratosphere by light absorbing particles, Geophys. Res. Lett., in press, 2004. 3487, 3488, 3498, 3499, 3500, 3510, 3527

Blake, D. F. and Kato, K.: Latitudinal distribution of black carbon soot in the upper troposphere and lower stratosphere, J. Geophys. Res., 100, 7195–7202, 1995. 3487, 3488, 3491, 3498, 3499, 3501, 3502, 3509, 3510, 3527

Brinkop, S. and Sausen, R.: A finite difference approximation for convective transports which maintains positive tracer concentrations, Beitr. Phys. Atmos., 3, 245–248, 1997. 3490

Chung, S. H. and Seinfeld, J. H.: Global distribution and climate forcing of carbonaceous aerosols, J. Geophys. Res., 107, (D19), 4407, doi:10.1029/2001JD001397, 2002. 3487, 3488, 3502

Cooke, W. F. and Wilson, J. J. N.: A global black carbon aerosol model, J. Geophys. Res., 101, 19 395–19 409, 1996. 3486, 3487, 3488, 3490, 3497, 3498, 3502

Cooke, W. F., Liousse, C., Cachier, H., and Feichter, J.: Construction of a 1°×1° fossil fuel emission data set for carbonaceous aerosol and implementation and radiative impact in the ECHAM4 model, J. Geophys. Res., 104, 22 137–22 162, 1999. 3486, 3487, 3488, 3490, 3501, 3502

Cooke, W. F., Ramaswamy, V., and Kasibhatla, P.: A general circulation model study of the global carbonaceous aerosol distribution, J. Geophys. Res., 107, (D16), doi:10.1029/2001JD001274, 2002. 3486, 3487, 3488, 3498, 3501, 3502

Danilin, M. Y., Fahey, D. W., Schumann, U., Prather, M. J., Penner, J. E., Ko, M. K. W., Weisenstein, D. K., Jackman, C. H., Pitari, G., Köhler, I., Sausen, R., Weaver, C. J., Douglass, A. R., Connell, P. S., Kinnison, D. E., Dentener, F. J., Fleming, E. L., Berntsen, T. K., Isaksen,

I. S. A., Haywood, J. M., and Kärcher, B.: Aviation fuel tracer simulation: Model intercomparison and implications, Geophys. Res. Lett., 25, 3947–3950, 1998. 3487, 3488, 3496, 3502, 3503, 3505, 3506

DeMott, P. J., Rogers, D. C., and Kreidenweis, S. M.: The susceptibility of ice formation in upper tropospheric clouds to insoluble aerosol components, J. Geophys. Res., 102, 19 575–19 584, 1997. 3487

Dibb, J. E., Talbot, R. W., and Loomis, M. B.: Tropospheric sulfate distribution during SUCCESS: Contribution from jet exhaust and surface sources, Geophys. Res. Lett., 25, 1375–1378, 1998. 3490, 3515

Dibb, J. E., Talbot, R. W., and Scheuer, E. M.: Composition and distribution of aerosols over the North Atlantic during the Subsonic Assessment Ozone and Nitrogen Oxide Experiment (SONEX), J. Geophys. Res., 105, 3709–3717, 2000. 3490, 3515

Döpelheuer, A.: Berechnung der Produkte unvollständiger Verbrennung aus Luftfahrttriebwerken, Inst. für Antriebstechnik, Deutsches Zentrum für Luft- und Raumfahrt, IB-325-09-97 Cologne, Germany, 1997. 3492

Döpelheuer, A.: Anwendungsorientierte Verfahren zur Bestimmung von CO, HC und Ruß aus Luftfahrttriebwerken, Ph.D. thesis, Deutsches Zentrum für Luft- und Raumfahrt, Report 2002-10, ISSN 1434-8454, Cologne, Germany, 109, 2002. 3492, 3508, 3524

Feichter, J., Kjellström, E., Rodhe, H., Dentener, F., Lelieveld, J., and Roelofs, G.-J.: Simulation of the tropospheric sulfur cycle in a global climate model, Atmos. Environ., 30, 1693–1707, 1996. 3490

Gierens, K.: On the transition between heterogeneous and homogeneous freezing, Atmos. Chem. Phys., 3, 437–446, 2003. 3487, 3511

Gierens, K., Schumann, U., Helten, M., Smit, H., and Wang, P.-H.: Ice-supersaturated regions and subvisible cirrus in the northern midlatitude upper troposphere, J. Geophys. Res., 105, 22 743–22 753, 2000. 3516

Haag, W., Kärcher, B., Ström, J., Minikin, A., Lohmann, U., Ovarlez, J., and Stohl, A.: Freezing thresholds and cirrus cloud formation mechanisms inferred from in situ measurements of relative humidity, Atmos. Chem. Phys., 3, 1791–1806, 2003. 3511

Haywood, J. M. and Ramaswamy, V.: Global sensitivity studies of the direct radiative forcing due to anthropogenic sulfate and black carbon aerosols, J. Geophys. Res., 103, 6043–6058, 1998. 3487

Hess, M., Köpke, P., and Schult, I.: Optical properties of aerosols and clouds: The software

package OPAC, Bull. Americ. Met. Soc., 79, 831–844, 1998. 3491
Hitzenberger, R., Berner, A., Giebl, H., Drobesch, K., Kasper-Giebl, A., Loeflund, M., Urban, H., and Puxbaum, H.: Black carbon (BC) in alpine aerosols and cloud water – concentrations and scavenging efficiencies, Atmos. Environ., 35, 5135–5141, 2001. 3490
Intergovernmental Panel on Climate Change (IPCC): Aviation and the Global Atmosphere, edited by Penner, J. E., Lister, D. H., Griggs, D. J., Dokken, D. J., and McFarland, M., Cambridge Univ. Press, New York, 1999. 3487, 3491, 3492, 3511, 3512
Jacobson, M. Z.: Control of fossil-fuel particulate black carbon and organic matter, possibly the most effective method of slowing global warming, J. Geophys. Res., 107, 4410, doi:10.1029/2001JD001376, 2002. 3487
Jensen, E. J. and Toon, O. B.: The potential impact of soot particles from aircraft exhaust on cirrus clouds, Geophys. Res. Lett., 24, 249–252, 1997. 3487, 3508
Kärcher, B.: Aviation-produced aerosols and contrails, Surveys in Geophysics, 20, 113–167, 1999. 3487, 3493, 3516
Kärcher, B. and Meilinger, S. K.: Perturbation of the aerosol layer by aviation-produced aerosols: A parametrization of plume processes, Geophys. Res. Lett., 25, 4465–4468, 1998. 3513
Kärcher, B. and Lohmann, U.: A parameterization of cirrus cloud formation: Heterogeneous freezing, J. Geophys. Res., 108, 4402, doi:10.1029/2002JD003220, 2003. 3487, 3508, 3511
Kjellström, E., Feichter, J., Sausen, R., and Hein, R.: The contribution of aircraft emissions to the atmospheric sulfur budget, Atmos. Environ., 33, 3455–3465, 1999. 3504
Koch, D.: Transport and direct radiative forcing of carbonaceous and sulfate aerosols in the GISS GCM, J. Geophys. Res., 106, 20 311–20 332, 2001. 3487, 3488, 3501, 3502
Köhler, I., Dameris, M., Ackermann, I., and Hass, H.: Contribution of road traffic emissions to the atmospheric black carbon burden in the mid-1990s, J. Geophys. Res., 106, 17 997–18 014, 2001. 3487, 3488, 3502
Köpke, P., Hess, M., Schult, I., and Shettle, E. P.: Global aerosol data set, Tech. Rep. 243, Max-Planck-Inst. für Meteorol., Hamburg, Germany, 44, 1997. 3491
Liousse, C., Penner, J. E., Chuang, C., Walton, J. J., Eddleman, H., and Cachier, H.: A global three-dimensional model study of carbonaceous aerosols, J. Geophys. Res., 101, 19 411–19 432, 1996. 3486, 3487, 3488, 3497, 3502
Lohmann, U. and Kärcher, B.: First interactive simulations of cirrus clouds formed

by homogeneous freezing in the ECHAM GCM, J. Geophys. Res., 107, 4105, doi:10.1029/2001JD000767, 2002. 3490
Lohmann, U. and Roeckner, E.: Design and performance of a new cloud microphysical scheme developed for the ECHAM general circulation model, Clim. Dyn., 12, 557–572, 1996. 3490
Lohmann, U., Feichter, J., Chuang, C. C., and Penner, J. E.: Prediction of the number of cloud droplets in the ECHAM GCM, J. Geophys. Res., 104, 9169–9198, 1999. 3490
Lohmann, U., Feichter, J., Penner, J. E., and Leaitch, W. R.: Indirect effect of sulfate and carbonaceous aerosols: A mechanistic treatment, J. Geophys. Res., 105, 12 193–12 206, 2000. 3487
Matta, E., Facchini, M. C., Decesari, S., Mircea, M., Cavalli, F., Fuzzi, S., Putaud, J.-P., and Dell'Acqua, A.: Mass closure on the chemical species in size-segregated atmospheric aerosol collected in an urban area of the Po Valley, Italy, Atmos. Chem. Phys., 3, 623–637, 2003. 3501
Minikin, A., Petzold, A., Ström, J., Krejci, R., Seifert, M., van Velthoven, P., Schlager, H., and Schumann, U.: Aircraft observations of the upper tropospheric fine particle aerosol in the Northern and Southern Hemispheres at midlatitudes, Geophys. Res. Lett., 30, 1503, doi:10.1029/2002GL016458, 2003. 3514
Myhre, G., Stordal, F., Restad, K., and Isaksen, I. S. A.: Estimation of the direct radiative forcing due to sulfate and soot aerosols, Tellus, 50B, 463–477, 1998. 3487
Neusüß, C., Pelzing, M., Plewka, A., and Herrmann, H.: A new analytical approach for size-resolved speciation of organic compounds in atmospheric aerosol particles: Methods and first results, J. Geophys. Res., 105, 4513–4527, 2000a. 3501
Neusüß, C., Weise, D., Birmili, W., Wex, H., Wiedensohler, A., and Covert, D. S.: Size-segregated chemical, gravimetric and number distribution-derived mass closure of the aerosol in Sagres, Portugal during ACE-2, Tellus, 52B, 169–184, 2000b. 3501
Neusüß, C., Wex, H., Birmili, W., Wiedensohler, A., Koziar, C., Busch, B., Brüggemann, E., Gnauck, T., Ebert, M., and Covert, D. S.: Characterization and parameterization of atmospheric particle number-, mass-, and chemical-size distributions in central Europe during LACE 98 and MINT, J. Geophys. Res., 107, 8127, doi:10.1029/2001JD000514, 2002. 3501
Penner, J. E., Eddleman, H., and Novakov, T.: Towards the development of a global inventory for black carbon emissions, Atmos. Environ., 27, 1277–1295, 1993. 3486
Penner, J. E., Chuang, C. C., and Grant, K.: Climate forcing by carbonaceous and sulfate aerosols, Clim. Dyn., 14, 839–851, 1998. 3487

Petzold, A., Ström, J., Ohlsson, S., and Schröder, F. P.: Elemental composition and morphology of ice crystal residual particles in cirrus clouds and contrails, Atmos. Res., 49, 21–34, 1998. 3487

Petzold, A., Döpelheuer, A., Brock, C. A., and Schröder, F. P.: In situ observations and model calculations of black carbon emission by aircraft at cruise altitude, J. Geophys. Res., 104, 22 171–22 181, 1999. 3492, 3498, 3508, 3513, 3514

Petzold, A., Fiebig, M., Flentje, H., Keil, A., Leiterer, U., Schröder, F., Stifter, A., Wendisch, M., and Wendling, P.: Vertical variability of aerosol properties observed at a continental site during LACE 98, J. Geophys. Res., 107, (D21), 8128, doi:10.1029/2001JD001043, 2002. 3514

Pruppacher, H. R. and Klett, J. D.: Microphysics of Clouds and Precipitation, Kluwer Acad., Dordrecht, The Netherlands, 954, 1997. 3515

Pueschel, R. F., Blake, D. F., Snetsinger, K. G., Hansen, A. D. A., Verma, S., and Kato, K.: Black carbon (soot) aerosol in the lower stratosphere and upper troposphere, Geophys. Res. Lett., 19, 1659–1662, 1992. 3487, 3488, 3498, 3499

Pueschel, R. F., Verma, S., Rohatschek, H., Ferry, G. V., Boiadjieva, N., Howard, S. D., and Strawa, A. W.: Vertical transport of anthropogenic soot aerosol into the middle atmosphere, J. Geophys. Res., 105, 3727–3736, 2000. 3491, 3509

Rahmes, T. F., Omar, A. H., and Wuebbles, D. J.: Atmospheric distributions of soot particles by current and future aircraft fleets and resulting radiative forcing on climate, J. Geophys. Res., 103, 31 657–31 667, 1998. 3487, 3488, 3503, 3505, 3506

Roeckner, E., Arpe, K., Bengtsson, L., Christoph, M., Claussen, M., Dümenil, L., Esch, M., Giorgetta, M., Schlese, U., and Schulzweida, U.: The atmospheric general circulation model ECHAM4: Model description and simulation of the present day climate, Tech. Rep., 218, Max–Planck–Inst. für Meteorol., Hamburg, Germany, 1996. 3489

Rogers, H., Teyssedre, H., Pitari, G., Grewe, V., van Velthoven, P., and Sundet, J.: Model intercomparison of the transport of aircraft-like emissions from sub- and supersonic aircraft, Meteorol. Zeitschrift, 11, 151–159, 2002. 3503, 3505

Schmitt, A. and Brunner, B.: Emissions from aviation and their development over time. In: Final Report on the BMBF Verbundprogramm, Schadstoffe in der Luftfahrt, edited by Schumann, U., Chlond, A., Ebel, A., Kärcher, B., Pak, H., Schlager, H., Schmitt, A., and Wendling, P., DLR-Mitteilung 97-04, Deutsches Zentrum für Luft- und Raumfahrt, Oberpfaffenhofen and Cologne, Germany, 37–52, 1997. 3491

Schröder, F. P., Kärcher, B., Petzold, A., Baumann, R., Busen, R., Hoell, C., and Schuman, U.: Ultrafine aerosol particles in aircraft plumes: In situ observations, Geophys. Res. Lett., 25, 2789–2792, 1998. 3516

Schröder, F., Kärcher, B., Fiebig, M., and Petzold, A.: Aerosol states in the free troposphere, J. Geophys. Res., 107, (D21), 8126, doi:10.1029/2001JD000194, 2002. 3513

Schult, I., Feichter, J., and Cooke, W.: Effect of black carbon and sulfate aerosols on the global radiation budget, J. Geophys. Res., 102, 30 107–30 117, 1997. 3487

Stephens, M., Turner, N., and Sandberg, J.: Particle identification by Laser Induced Incandescence in a solid state laser cavity, Appl. Optics, 42, 3726–3736, 2003. 3500

Strawa, A. W., Drdla, K., Ferry, G. V., Verma, S., Pueschel, R. F., Yasuda, M., Salawitch, R. J., Gao, R. S., Howard, D. D., Bui, P. T., Loewenstein, M., Elkins, J. W., Perkins, K. K., and Cohen, R.: Carbonaceous aerosol (Soot) measured in the lower stratosphere during POLARIS and ist role in stratospheric photochemistry, J. Geophys. Res., 104, 26 753–26 766, 1999. 3491, 3499, 3509

Ström, J. and Ohlsson, S.: In-situ measurements of enhanced crystal number densities in cirrus clouds caused by aircraft exhaust, J. Geophys. Res., 103, 11 355–11 361, 1998. 3487, 3506

Williamson, D. L. and Rasch, P. J.: Water vapor transport in the NCAR CCM2, Tellus, 46A, 34–51, 1994. 3489

Table 1. Summary of model runs.

Experiment	Description
BASE	standard simulation, τ_{BC}=24 h
PHIL	as BASE, but BC generally hydrophilic
PHOB	as BASE, but τ_{BC}=48 h
NOICE	as BASE, but scavenging of aerosols by cloud ice is neglected above the 400 hPa level.

τ_{BC} : = e-folding time for transformation of hydrophobic to hydrophilic BC.

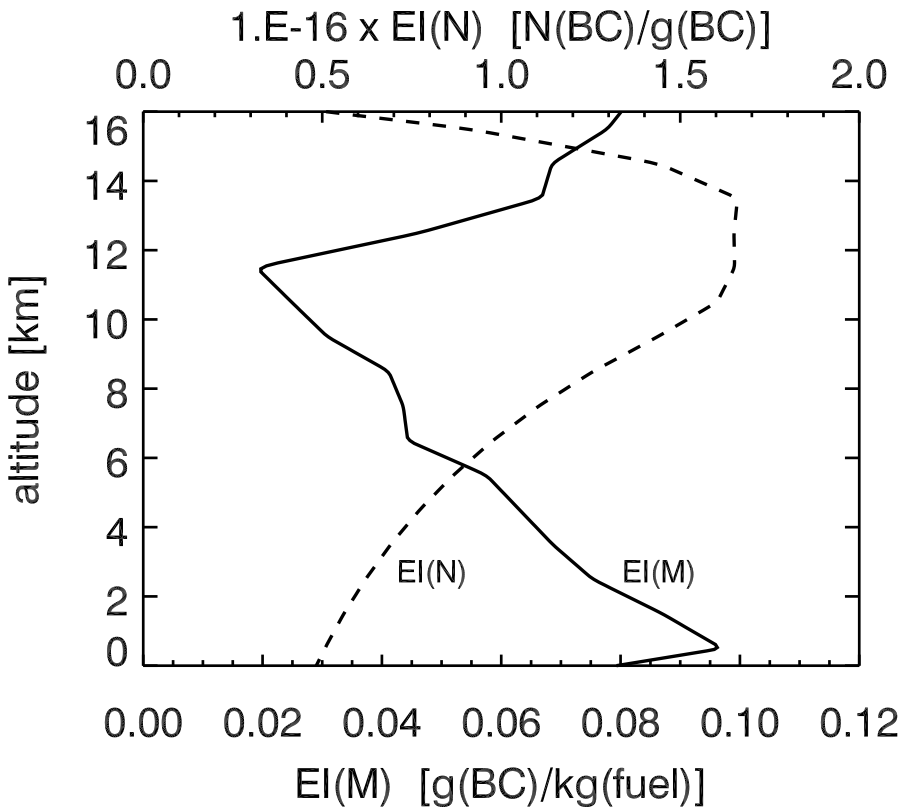

Fig. 1. Vertical profiles of aircraft emission indices for the BC mass (solid) and particle number concentration (dashed), representative of the 1992 aircraft fleet. For details see Sect. 2.3 and Döpelheuer (2002).

ACPD
4, 3485–3533, 2004

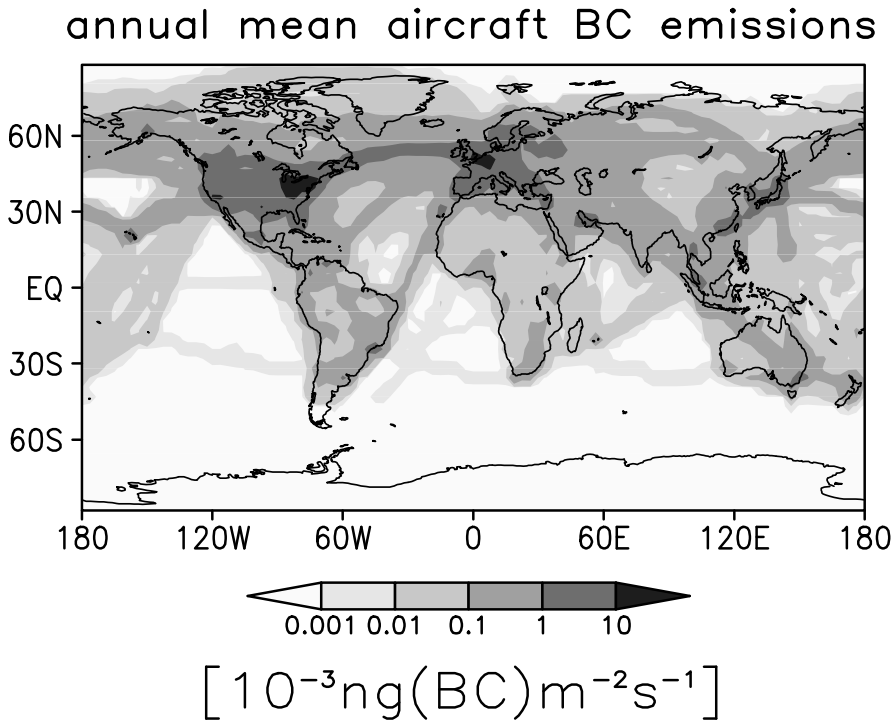

Fig. 2. Annual mean vertically integrated BC emissions due to aviation. The emission rates were derived from aviation fuel consumption data and emission indices for the 1992 global fleet (see Sect. 2.3 for details).

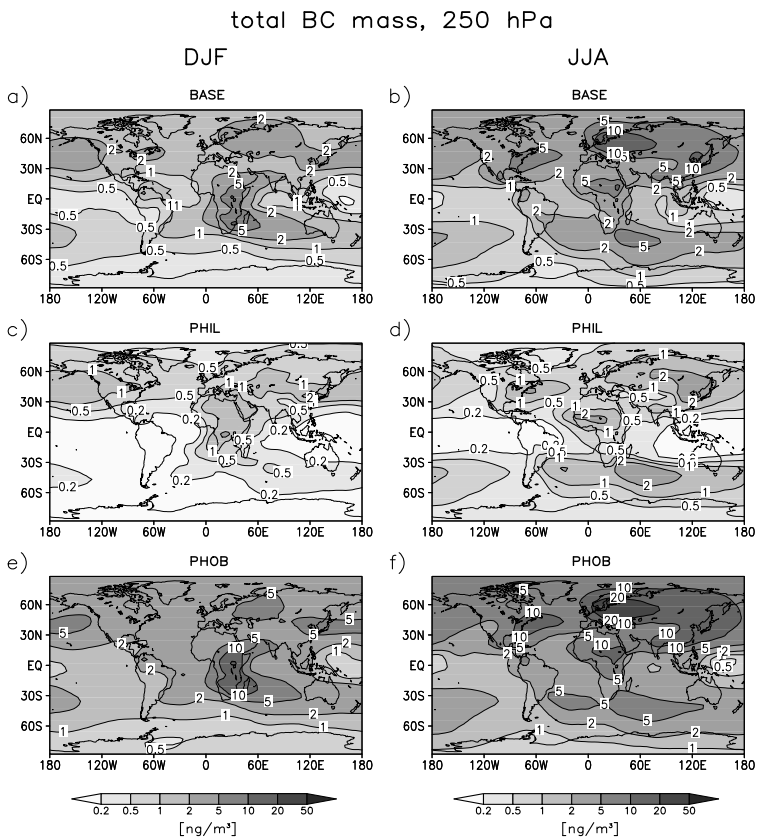

Fig. 3. Total BC mass concentration (ng/m^3) at 250 hPa (main aircraft flight level) during northern hemispheric (NH) winter (left) and summer (right) simulated in the experiments BASE **(a, b)**, PHIL **(c, d)** and PHOB **(e, f)**. The results represent 4-year averages of the December to February and the June to August periods, respectively.

ACPD
4, 3485–3533, 2004

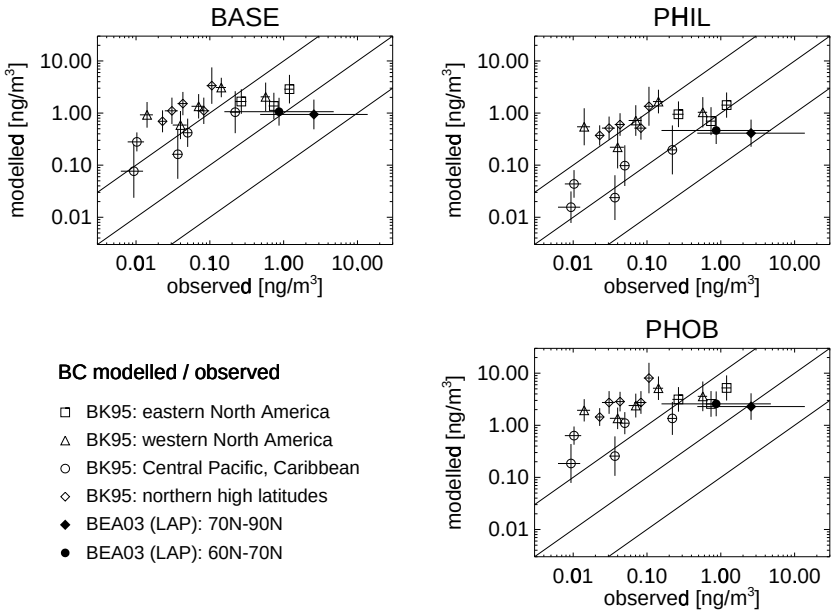

Fig. 4. Comparison of simulated UTLS BC concentrations with in-situ observations of BC (Blake and Kato, 1995, referred to as BK95) and light absorbing particles (LAP)(Baumgardner et al., 2003, 2004, referred to as BEA03). Simulated BC concentrations (ng/m^3) are plotted against observed values. The simulated BC values represent median concentrations and standard deviations (variability of 12-h averages) extracted from the 4-year model output for the geographical positions, altitudes, and months corresponding to the respective observations. Data is shown for the different cases BASE (top left), PHIL (top right) and PHOB (bottom right). Observed values are local values and their uncertainties (BK95) or median values and standard deviations (BEA03). Equity of simulations and observations as well as deviations by one order of magnitude are indicated by diagonal lines. Only measurements performed between 5 and 15 km altitude were considered. Since the original observational data are normalized to standard (STP) conditions, the data has been adjusted to local conditions. See Sect. 3.2.2 for more details.

ACPD
4, 3485–3533, 2004

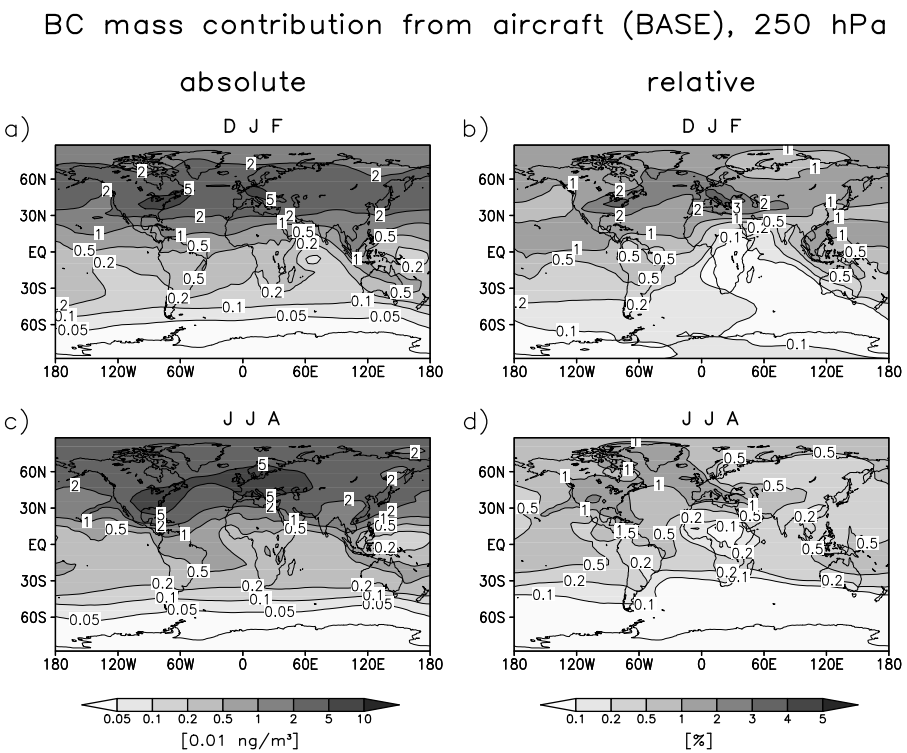

Fig. 5. Contribution of aviation to the BC mass concentration at 250 hPa (main flight level) during NH winter **(a, b)** and summer **(c, d)** as simulated in the BASE experiment. Absolute contributions (0.01 ng/m^3)(a, c) and relative contributions (% of total BC mass)(b, d) are displayed. The results represent 4-year averages of the December to February and the June to August periods, respectively.

ACPD
4, 3485–3533, 2004

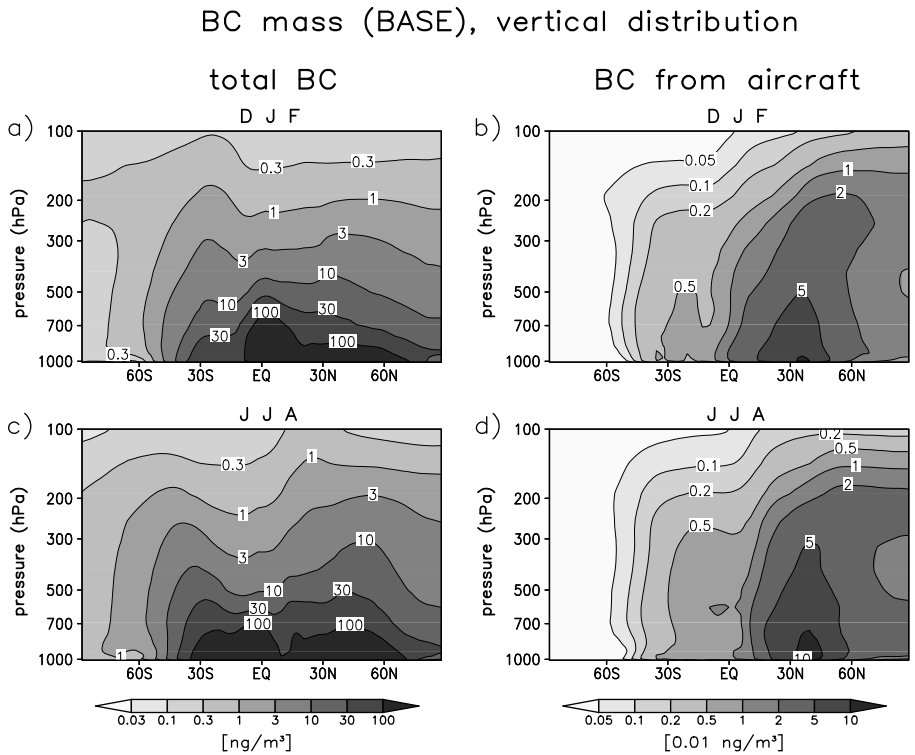

Fig. 6. Left: Vertical distribution of zonal mean total BC mass concentration (ng/m^3) during NH winter **(a)** and summer **(c)** simulated in the BASE experiment. Right: Corresponding BC contribution of aviation (0.01 ng/m^3)**(b, d)**. The displayed concentrations represent 4-year averages of the December to February and the June to August periods, respectively.

ACPD
4, 3485–3533, 2004

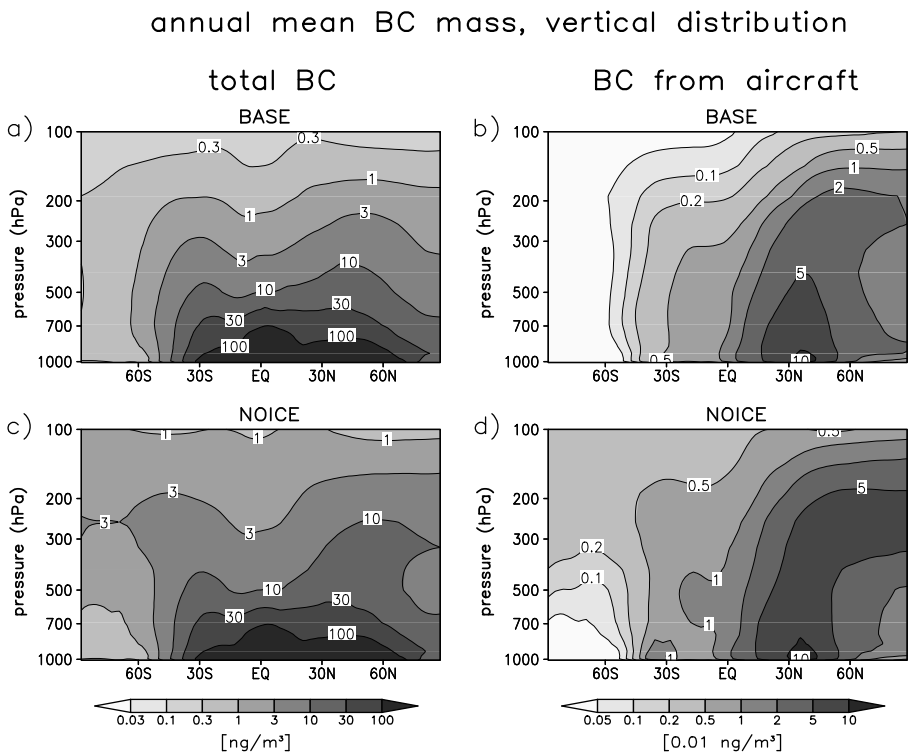

Fig. 7. As Fig. 6, but annual mean BC mass concentrations obtained in the BASE **(a, b)** and NOICE **(c, d)** simulations.

ACPD
4, 3485–3533, 2004

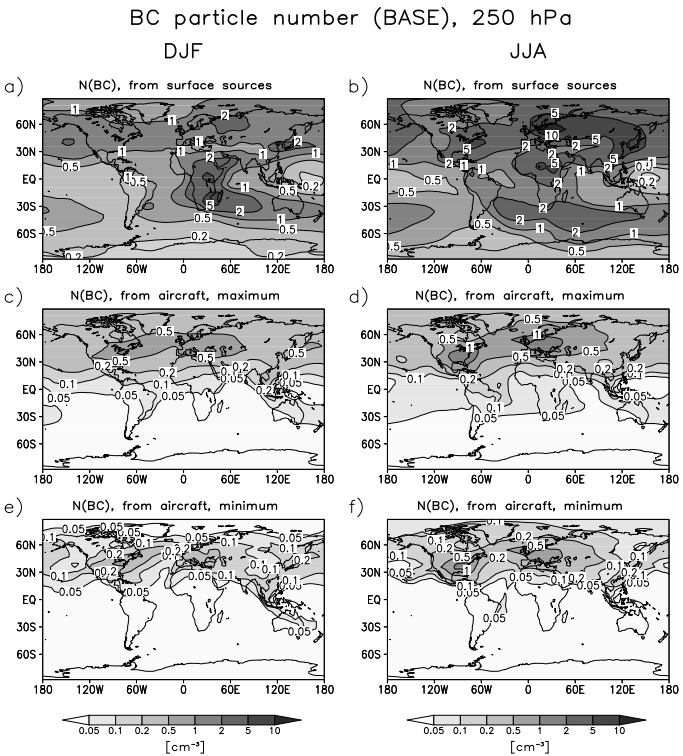

Fig. 8. Particle number concentrations (cm^{-3}) of BC at 250 hPa (main aircraft flight level) during NH winter (left) and summer (right) simulated in the BASE experiment. **(a, b)**: Number concentrations of BC particles resulting from surface sources. **(c–f)**: Number concentrations of aviation-induced BC particles obtained when ageing of aviation BC (see Sect. 2.4, Appendix) is neglected (c, d) and when efficient ageing of aviation BC is considered (e, f). The displayed concentrations represent 4-year averages of the December to February and the June to August periods, respectively.

ACPD
4, 3485–3533, 2004

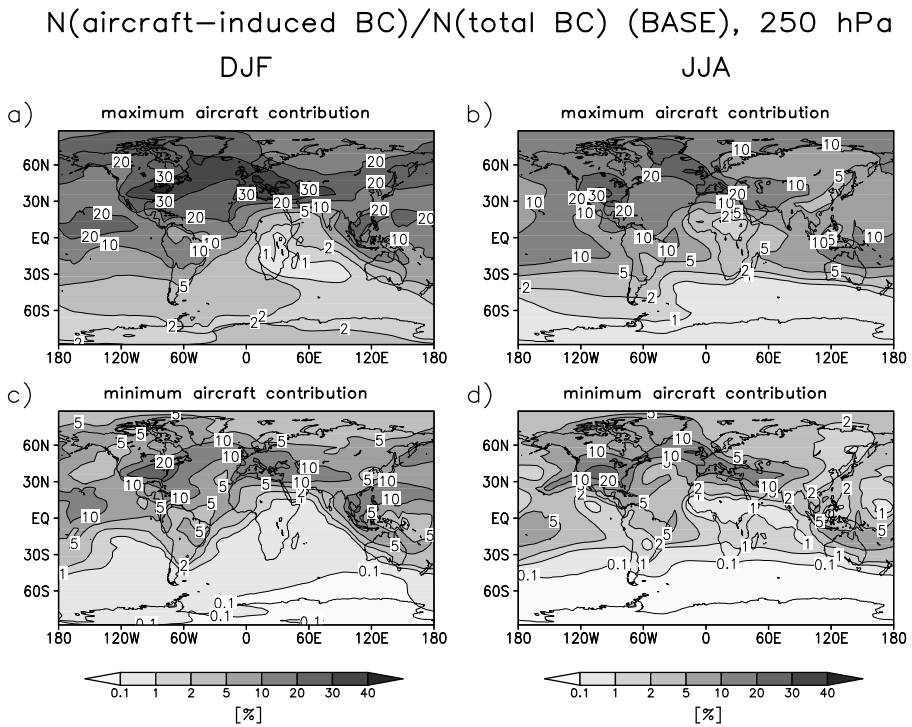

Fig. 9. Relative contribution (%) of BC from aviation to the total BC particle number concentration at 250 hPa (main aircraft flight level) during NH winter (left) and summer (right) simulated in the BASE experiment. **(a, b)**: Ageing of aviation BC (see Sect. 2.4, Appendix) is neglected. **(c, d)**: Efficient ageing of aviation BC is considered. The displayed contributions represent 4-year averages of the December to February and the June to August periods, respectively.

ACPD
4, 3485–3533, 2004

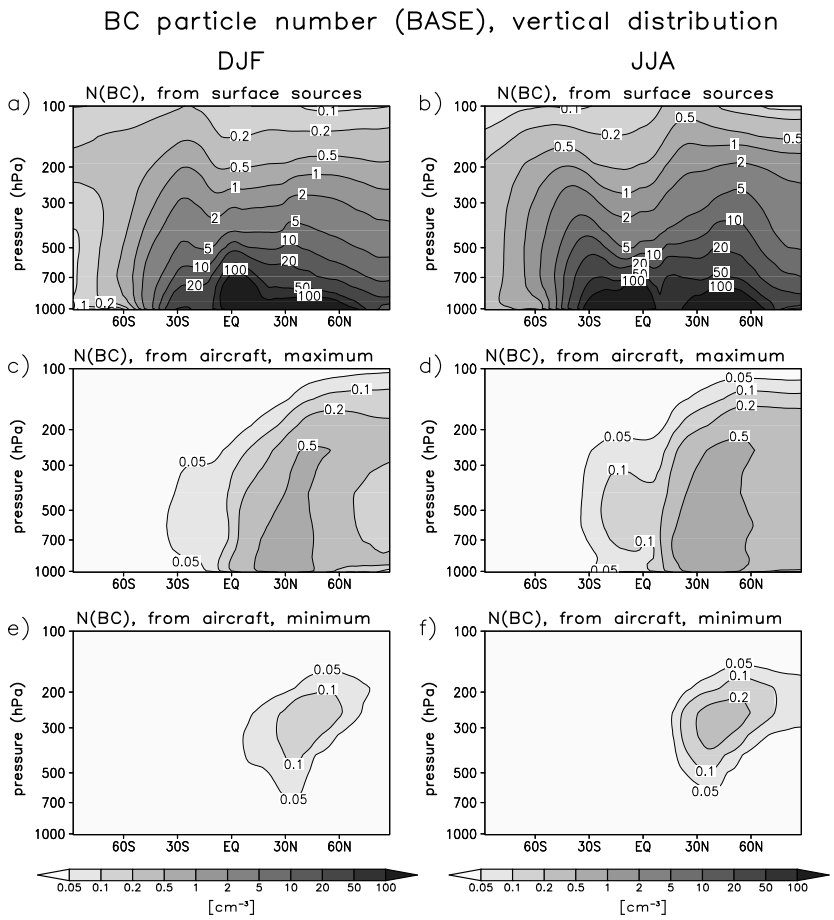

Fig. 10. As Fig. 8, but vertical distributions of zonal mean BC particle number concentrations (cm^{-3}) are highlighted.

ACPD
4, 3485–3533, 2004